

CWRU-P7-94
SEPT 1994

YET ANOTHER PAPER ON SN1987A: LARGE ANGLE OSCILLATIONS, AND THE ELECTRON NEUTRINO MASS

Peter J. Kernan and Lawrence M. Krauss¹

*Department of Physics
Case Western Reserve University
10900 Euclid Ave., Cleveland, OH 44106-7079*

Abstract

We supplement Maximum Likelihood methods with a Monte-Carlo simulation to re-investigate the SN1987A neutrino burst detection by the IMB and Kamiokande experiments. The detector simulations include background in the the latter and “dead-time” in the former. We consider simple neutrinosphere cooling models, explored previously in the literature, to explore the case for or against neutrino vacuum mixing and massive neutrinos. In the former case, involving kinematically irrelevant masses, we find that the full range of vacuum mixing angles, $0 \leq \sin^2 2\theta_V \leq 1$, is permitted, and the Maximum Likelihood mixing angle is $\sin^2 2\theta_V = .45$. In the latter case we find that the inclusion of “dead-time” reduces previous m_{ν_e} upper bounds by 10%, and supplementing the Maximum Likelihood analysis with a Monte-Carlo goodness-of-fit test results in a further 15% reduction in the m_{ν_e} upper limit. Our 95% C.L. upper limit for m_{ν_e} is 19.6eV, while the best fit value is ~ 0 eV.

¹Also Dept of Astronomy

Introduction

Galactic neutrino astronomy began in 1987 with the observation of 20 neutrinos from the supernovae burst SN1987A in the Large Magellanic Cloud (LMC). Two terrestrial detectors, IMB [1] and Kamiokande [2], found unequivocal evidence for supernovae neutrino events with the former collaboration claiming detection of 8 SN1987A events, and the latter 12. This momentous observation generated enormous excitement in the scientific community, and of course a plethora of papers soon followed. We have returned to this subject for three reasons. First, apparently only the IMB collaboration took into account the “dead-time” in the IMB detector when comparing these observations with theory. Also we believe that a more or less model-independent approach to the question of vacuum mixing in SN1987A should be done (and with more rigor than in [3]). Finally, we have in hand a detailed Monte Carlo code for generating the predicted signal in light water detectors which was created for the purpose of exploring the nature of a galactic neutrino signal [4], but which can also be used to accurately model the signal for SN1987A. Using this code we felt that it might be possible to improve upon the neutrino mass limits derived previously for the SN1987A neutrino burst.

Before describing our analysis, it is worthwhile briefly reviewing the most recent results on neutrino mass and mixing constraints from SN1987A in order to comment on the improvements incorporated in our present analysis. To date, the most comprehensive statistical analysis of the signal was performed by Lamb and Loredo [5], who used a Maximum Likelihood technique, and were the first to incorporate the background event rate in a likelihood function in order to account for at least one of the Kamiokande events which

was probably a background event (which several previous analyses had simply discarded). To facilitate comparison with their results (in the case of a significant neutrino mass) we exploited essentially the same formalism, but made several minor additions. Primarily, we included the fact that the IMB detector had a significant amount of “dead-time” ($\sim 13\%$ over the burst [1]) following interactions in the detector by cosmic ray muons or SN1987A neutrinos. The reason for the large dead-time, 35ms/interaction, is due to the data-acquisition software [6]. This 35ms dead-time would of course not be problematic for the original purpose of the IMB detector, measuring proton decay.

A few investigators [5, 7] allowed *independent* offset times (the time-delay between the first SN1987A neutrino arriving at the earth and the first detection in either Kamiokande or IMB) for each detector. We noticed that in the case of a significant neutrino mass, when the offset times, t_{off} , are important, the Maximum Likelihood value t_{off}^{kam} (Kamiokande offset time) at the m_{ν_e} upper limit of Lamb and Loredo seemed unacceptably long. This suggested extending the Maximum Likelihood approach. The Maximum Likelihood method does not test a model, but rather tests the allowed range of parameters given a specific model. Thus should the Maximum Likelihood method locate a parameter value which may seem otherwise unlikely one must use other methods, such as a Monte-Carlo, to test the model. Here we were able to exploit the power of the comprehensive light water neutrino detector Monte Carlo code previously written to examine various features of possible future galactic neutrino burst signals [4]. This code incorporates all aspects of the detector in order to generate a realistic signal, given a specific

supernova burst model. Using this Monte Carlo, we can show, as we describe in more detail below, that the Lamb and Loredó Maximum Likelihood offset time for Kamiokande of 3.9 sec would be expected to occur in less than 1 out of 400 cases given the other Maximum Likelihood SN1987A parameters, such as binding energy, emission timescale, etc.

We next turn to the issue of neutrino mixing constraints. There has recently been a model-dependent derivation of bounds on vacuum oscillations from the SN1987A data [8], with 5 specific explosion models considered. All models fit the no-mixing scenario and, perhaps not surprisingly, when the amount of neutrino mixing was increased a Kolmogorov-Smirnov test led to a lower bound of $\sin^2 2\theta_V < .7 \rightarrow .9$. The upper bound of .7 would exclude the “just-so” solution [9] to the solar neutrino problem [10] and much of the large angle region of the MSW solution. The severity of this bound is surprising, given the sparsity of the observed signal, so we decided to examine this issue in some more detail. The authors of [8] recognized the fact that their result was model dependent, but just how model dependent was not clear. The ability to explore the neutrino signal with our Monte Carlo makes it very easy to sample supernova model space. We will show below that with a minimally model-dependent approach, maximal vacuum mixing actually fits the data better (greater likelihood) than no mixing.

Finally, we note that the neutrino mass limit we derive here has already been superceded by direct laboratory probes [11]. Nevertheless, the utility of exploiting a galactic supernova burst to constrain neutrino masses and mixings remains of great interest, and the techniques we examine here thus remain important to explore. Namely, SN1987A remains, even 7 years later,

an important, and unique test case if we are to attempt to fully exploit the information which may be available in the next observed supernova neutrino burst.

The Minimal Model

We exploit here two “minimal” models. The version we use for bounding the neutrino mass and the one used for bounding the vacuum mixing angle differ in that the latter has an extra time constant in the neutrino spectra, which we will discuss later. In the former case we follow Lamb and Loredò and assume a simple exponential cooling model. In this case the supernovae is characterized by a Fermi-Dirac neutrino spectrum and 3 parameters; a maximum initial temperature $T_{\bar{\nu}_e}^0$, a cooling time-scale τ_c , and α , related to the size of the neutrinosphere,

$$\alpha = \frac{R_{10}}{D_{50}}. \quad (1)$$

With R_{10} the radius of the neutrinosphere in units of 10 kilometers and D_{50} the distance to the LMC in units of 50 kiloparsecs. Alternatively one can view α as a relation for the supernovae binding energy with the additional assumption that there is an equipartition of the binding energy carried away among the 3 flavor states times 2 spin states of the emitted neutrinos.

$$E_{53} = 3.39 \times 10^{-4} \alpha^2 D_{50}^2 \int T_{\bar{\nu}_e}^4(t) dt \quad (2)$$

with E_{53} the neutron star binding energy in units of 10^{53}ergs and $T_{\bar{\nu}_e}$ given in the simple exponential cooling model by

$$T_{\bar{\nu}_e}(t) = T_{\bar{\nu}_e}^0 \exp(-t/4\tau_c). \quad (3)$$

The model is also characterized by the neutrino mass, m_{ν_e} , and an additional parameter for each detector, t_{off} , the offset time. The offset time is particularly important for the massive neutrino case where the neutrino mass causes a delay-time in the arrival of the neutrinos:

$$\Delta t = 2.57(m_{\nu_e}^2)_{eV^2} E_{MeV}^{-1} D_{50s}, \quad (4)$$

with m_{ν_e} in units of eV and E_{MeV} , the incident neutrino energy, in MeV. Independent offset times are needed for each detector [7] because of a problem with the Kamiokande clock during the time that the SN1987A neutrino burst passed the earth. The offset times play a major role in constraining non-zero neutrino masses, due to the difficulty, when maximizing the likelihood function for the Kamiokande detector, of reconciling a few early low energy neutrino events, which would then imply a large offset time for non-zero mass, with following high energy events, which would favor a small offset time [12].

The second version of our minimal model, in the case of vacuum mixing and nearly massless neutrinos, introduces an additional parameter for the anti-neutrino temperature, $T_{\bar{\nu}_e}$. As far as kinematics are concerned, in this part of the analysis we assume effectively massless neutrinos (the time delays introduced by the very small masses of interest in this case are irrelevant), and we assume two state mixing, ν_e and ν_μ . Vacuum mixing implies the neutrino spectrum at the earth is a mixture of the 2 original spectra according to

$$d^2N^{inc}/dEdt = (1 - .5 \sin^2 2\theta_V)d^2N^{\bar{\nu}_e}/dEdt + .5 \sin^2 2\theta_V d^2N^{\bar{\nu}_\mu}/dEdt \quad (5)$$

Qualitative arguments suggest that $T_{\nu_\mu} \simeq 2T_{\nu_e}$ due to the fact that the ν_e have additional interactions from neutrons and charged current interactions, while ν_μ has only neutral-current interactions in the supernovae environment. Thus the ν_μ are emitted from deeper in the star and hence their spectrum is characterized by a hotter temperature. The temperature evolution of the $\bar{\nu}_e$ is potentially slightly more complicated: initially before neutronization of the star $T_{\bar{\nu}_e} \simeq T_{\nu_e}$ is expected. However as the star neutronizes and the reaction $\bar{\nu}_e + p \rightarrow n + e^+$ becomes rare then $T_{\bar{\nu}_e} \rightarrow T_{\nu_\mu}$ is expected [13]. Our model parameterizes this phenomenon by introducing an additional time-constant which smoothly and symmetrically takes $T_{\bar{\nu}_e}$ from T_{ν_e} to $T_{\nu_\mu} = 2T_{\nu_e}$ in time $2\tau_2$.

$$T_{\bar{\nu}_e} = \{1. + .5 \tanh [(t - \tau_2)\pi/\tau_2]\} T_{\nu_e}(t) \quad (6)$$

This function is constructed so that when t advances to τ_2 we have $T_{\bar{\nu}_e} = .5(T_{\nu_e} + T_{\nu_\mu})$. Introducing the extra parameter, τ_2 , allows us to take a conservative approach to the consideration of vacuum oscillations. Also we take T_{ν_e} and T_{ν_μ} to have the form of eq.3 (such that if the Maximum Likelihood $\tau_2 \gg \tau_c$ this will reduce $T_{\bar{\nu}_e}$ to the form used for massive neutrinos).

Another point worth mentioning here is that we continue to partition the binding energy equally among all species here so that the factor α , which sets the scale of the fluxes,

$$d^2N/dEdt \propto \alpha^2$$

is different for the 3 species, $\nu_e, \bar{\nu}_e$ and ν_μ . These are related by,

$$\alpha_{\nu_i} = \alpha_{\nu_e} \sqrt{\left(\int T_{\nu_e}^4 dt / \int T_{\nu_i}^4 dt \right)} \quad (7)$$

with $\nu_i = \bar{\nu}_e, \nu_\mu$.

As we have indicated, an improvement in our Maximum Likelihood method compared to the Lamb and Loredo work is the inclusion of dead-time for the IMB detector. The reason one expects this may have an effect is due to the fact that the Kamiokande data favors a cooler, less energetic supernovae than does the IMB data. Our Monte-Carlo work indicates that if one uses the IMB data to locate a set of SN1987A parameters, these same parameters typically predict many more events in Kamiokande ~ 20 , with a much higher average energy $\sim 22MeV$, than were seen (12 events and 15 MeV, respectively). Thus one of the reasons why the Maximum Likelihood analysis can provide a reasonably localized parameter space for the combination of the IMB and Kamiokande data is the tension between the fits for the two separate data sets. Since including the dead-time in IMB will favor an even more energetic supernovae it should exacerbate the existing tension leading to stronger constraints on parameters derived from the Maximum Likelihood method. One of the purposes of this letter is to show how much the 13% dead-time changes our conclusions from those of Lamb and Loredo .

The dead-time, $t_d = 35ms$, was handled in different ways in the Monte-Carlo and Maximum Likelihood methods. In the prior case it is straightforward. We use a Poisson distributed random number generator to simulate the known 2.7Hz muon event rate (this requires a 3Hz incident rate since dead-time affects this measurement as well) starting at $t - 1sec$. With the

Monte-Carlo neutrino events and muon events in temporal order we then remove any neutrino events occurring within 35ms of a previously “detected” muon or neutrino.

For the Maximum Likelihood method, we modify the spectral rate according to,

$$d^2N/dEdt \rightarrow (1 - P_d(t - t_d, t))d^2N^0/dEdt \quad (8)$$

where $P_d(t - t_d, t)$ is the probability that either a muon event or a neutrino event occurred in the interval from $t - t_d$ to t and $d^2N^0/dEdt$ is the spectral rate without deadtime. The probability, P_d , of an interaction which causes deadtime is decomposed as follows $P_d = P_{d\mu}P_{d\nu}$, using the poisson probability that there were 0 events from $t - t_d \rightarrow t$, assuming a rate Γ .

$$P_d = 1 - \exp(-\Gamma\delta t) \quad (9)$$

For the muons $\Gamma_\mu = 3Hz$, $\delta t = 35ms$. We approximate the neutrino induced dead time probability by evaluating the zeroth order contribution of the neutrinos to P_d at $t - t_d/2$, approximating $d^2N^0/dEdt$ as constant during that short interval. Since $t_d \ll \tau_c$ this is a good approximation. Thus, $\Gamma_\nu \propto dN_\nu^0$ and $\delta t = \min(t, t_d)$.

The data in our Maximum Likelihood code not specifically mentioned above, such as fiducial detector volumes, the parameters of the detector resolution functions, the energies and times of the background events in Kamiokande, follow the treatment in Lamb and Loredano, and are not repeated here. We use the standard likelihood function, see for example [4, 5].

The Monte-Carlo program is a modified version of the one described in [4]. The parameters which describe the detector efficiencies, resolution functions, the form of the neutrino temperature etc, have been set to be identical to the ones for the Maximum Likelihood analysis. This code (originally designed for O(1000) events) is fairly sophisticated and includes the interactions of neutrinos other than $\bar{\nu}_e$, and neutrino scattering from oxygen nuclei in the detector. The additional types of interactions in this code, and the more careful treatment of the dominant reaction $\bar{\nu}_e p \rightarrow n e^+$, which includes nucleon recoil effects, results in a small increase, $\sim 3\%$, in $\langle N \rangle$ compared to the Maximum Likelihood code estimate. The difference is insignificant for the SN1987A events however, as will become obvious.

Analysis of Results

(a) Massive Neutrinos

We first consider the limits on massive neutrinos. The initial step is to find the best fit Maximum Likelihood parameters for $\alpha, T_{\nu_e}^0, \tau_c, t_{off}^{kam}$ and t_{off}^{imb} as a function of m_{ν_e} . The effect of this procedure is to project the log likelihood onto the m_{ν_e} axis. From this projection, shown in Figure 1, we can find the 95% confidence limit from,

$$\ln \mathcal{L}^{Max} - .5\chi_{dof}^2(.05), \quad (10)$$

where we have 6 degrees of freedom (*dof*) for the chi-squared distribution in the present instance. We will denote the Maximum Likelihood value of a parameter by adding the subscript L^+ , and the value of a parameter at the 95% confidence boundary with some or all (which will be clear from the context) of the other parameters at their Maximum Likelihood values by

adding the subscript L^- . In this notation, from Figure 1,

$$(m_{\nu_e})_{L^+} = 0eV \quad (11)$$

$$(m_{\nu_e})_{L^-} = 23eV. \quad (12)$$

The likelihood function is extremely flat below $m_{\nu_e} = 2eV$ so this result does not strongly favor an identically zero neutrino mass. Our value for $(m_{\nu_e})_{L^-}$ is 8% lower than the Lamb and Loredò result $(m_{\nu_e})_{L^-} = 25eV$, the entire difference being due to the dead-time correction in our IMB likelihood function.

There is an additional constraint we may use in the analysis. Consider Figure 2 wherein $(t_{off}^{kam})_{L^+}$ and $(t_{off}^{imb})_{L^+}$ are shown as a function of m_{ν_e} (with $(\tau_c)_{L^+}$ included for comparison). Note that $(t_{off}^{kam})_{L^+}$ reaches 4.2s at $m_{\nu_e} = 23eV$ (where $(t_{off}^{imb})_{L^+} = 1s$). The Maximum Likelihood offset time for Kamiokande seems extraordinarily long, especially in light of the fact that $(t_{off}^{kam})_{L^+}$ exceeds $(\tau_c)_{L^+}$ for $m_{\nu_e} > 21.7eV$.

To test our intuition in this regard, and to discover the acceptable range of t_{off}^{det} one can use our Monte-Carlo code to find, given $(\alpha)_{L^+}$, $(T_{\bar{\nu}_e}^0)_{L^+}$ and $(\tau_c)_{L^+}$, for a particular m_{ν_e} , the probability, $P(t_{off}^{det} < t | N^{det}, m_{\nu_e})$, that the offset time in a particular detector will not exceed a certain value.

Note that we are interested in values of the mass parameter in the range $(m_{\nu_e})_{L^+}(0eV) < m_{\nu_e} < (m_{\nu_e})_{L^-}(23eV)$. We thus first determine, using the Maximum Likelihood method, $(t_{off}^{kam})_{L^-}$, the minimum acceptable t_{off}^{kam} , subject to the m_{ν_e} constraint with all the other parameters free. This is displayed in Figure 3. Then we use our Monte-Carlo to construct $P(t_{off}^{kam} < t | N^{kam}, m_{\nu_e})$. If we find that $(t_{off}^{kam})_{L^-}$ is ruled out at the 95% CL by this probability distribution, this then implies, since the likelihood function rules

out any smaller offset time, that the m_{ν_e} corresponding to this value is at least as unacceptable at this level.

We finally turn to the construction of $P(t_{off}^{kam} < t | N^{kam}, m_{\nu_e})$. Recall that in our detector simulation we include dead-time for IMB and background for Kamiokande. Also note that the time of the first event depends (more strongly as the number of events is decreased) on the number of events detected, and that this number is not fixed by our Monte-Carlo code, which temporally simulates the neutrino burst and detection. Therefore we require Monte-Carlo runs which result in the desired number of events for each detector. Then we rank the times of the first event of each such run and generate a cumulative probability distribution for the time of the first event. To improve the statistics, while conserving computer time, we choose a range, $N = N^{det} \pm 1$, about the desired number of events. (For this purpose $N^{kam} = 16$, including background, and $N^{imb} = 8$.) (Both detectors, for the parameters of interest here, have a flat distribution for the expected time of the first event in the neighborhood of the number of events actually observed.) We use 1000 Monte-Carlo runs of each detector to acquire the data for the construction of $P(t_{off}^{det} < t | N^{det}, m_{\nu_e})$. Typically about 20 – 30% of the Monte-Carlo runs fall in the accepted range of N^{det} .

In Figure 4a we plot $P(t_{off}^{det} < t | N^{det}, 21eV)$. Also shown are $(t_{off}^{kam})_{L+}$, and $(t_{off}^{imb})_{L+}$, for $m_{\nu_e} = 21eV$. Note that while $(t_{off}^{imb})_{L+} = .9s$ is located near the mean of the distribution, $(t_{off}^{kam})_{L+} = 3.8s$ is in the tail. In Figure 4b $P(t_{off}^{Kam} < t | N^{Kam}, 19.6eV)$ is plotted with $(t_{off}^{kam})_{L+}$ and $(t_{off}^{kam})_{L-}$ indicated. Since $(t_{off}^{kam})_{L-} > t^*$, where t^* is defined by $P(t_{off}^{kam} < t^* | N^{kam}, 19.6eV) = .95$, $m_{\nu_e} \geq 19.6eV$ is excluded at the 95% confidence level.

We thus find an additional decrease of 15% in the m_{ν_e} upper limit derivable using the Monte-Carlo generated probability $P(t_{off}^{kam} < t | N^{kam}, m_{\nu_e})$ in addition to the Maximum Likelihood procedure. This is a significant factor, and further underscores the utility of Monte Carlo simulation of the data. When combined with the effect of incorporating deadtime in the IMB detector, which fortuitously plays a significant role because of the paucity of observed events in Kamiokande, we have been able to reduce the upper limit on the m_{ν_e} mass by over 25% compared to previous analyses.

(b) Vacuum Mixing and Nearly Massless Neutrinos

Next we turn to our results for vacuum mixing. In this case the Maximum Likelihood values for the offset times are 0 for all values of $\sin^2 2\theta_V$, therefore we do not have to Monte-Carlo the neutrino burst. In Figure 5 $\ln \mathcal{L}(\sin^2 2\theta_V)$ is displayed for the range $0 \leq \sin^2 2\theta_V \leq 1$. (We ran the Maximum Likelihood code with and without including the offset times. The difference in $\ln \mathcal{L}$ never exceeded .02%. Thus the offset times are irrelevant parameters, and we consider only 5 *dof.*) In Figure 5 the likelihood function peaks at $\sin^2 2\theta_V = .45$. However, the likelihood function is relatively flat over the entire range so non-zero mixing is only marginally preferred. The likelihood ratio for $\sin^2 2\theta_V = 0.45$ compared to $\sin^2 2\theta_V = 0$ is 5.5.

Also of interest, perhaps to supernovae model builders, is our Maximum Likelihood extraction of neutrinosphere temperatures. In Figure 6a-c we display $T_{\nu_e}, T_{\bar{\nu}_e}$ and T_{ν_μ} for $\sin^2 2\theta_V = 0, .45$ and 1 respectively. The main feature is that in all cases $T_{\bar{\nu}_e} \rightarrow T_{\nu_\mu}$ gradually, with $\tau_2 = 9.13, 8.72$ and 8.35 respectively. This long timescale is something of a surprise.

A final question is whether the admission of constraints on SN1987A pa-

rameters, other than those purely obtainable from the neutrino data alone, would allow one to further limit $\sin^2 2\theta_V$. In Figure 7a-c we show: the Maximum Likelihood neutron star binding energy, E_{53}^B , in units of 10^{53} ergs; the initial electron neutrino temperature, $T_{\nu_e}^0$, in MeV; and the cooling time-scale, τ_c , in seconds. The entire range of the latter seems acceptable based on estimates from supernova models. One may ask whether constraints such as $E_{53}^B < 4.5$ or $T_{\nu_e}^0 > 3\text{MeV}$, would limit $\sin^2 2\theta_V$. From Figure 7 it appears that this could be the case.

To address this question we find the 95% confidence level regions in the $E_{53}^B, T_{\nu_e}^0$ plane for several values of $\sin^2 2\theta_V$. The remaining parameters are all permitted to find their Maximum Likelihood values². In Figure 8 we display the results for 6 values of $\sin^2 2\theta_V$ from .1 to 1. The outer contour in each box is the 95% confidence limit (5 degrees of freedom), while the inner contours; 50%, 25%, and 10% C.L. , are shown to allow the reader to assess the character of the surface. It is apparent from Figure 8 that no reasonable E_{53}^B provides a further solid constraint on $\sin^2 2\theta_V$.

We have constructed Table 1 to present the maximum allowed $\sin^2 2\theta_V$ at 95% confidence level in terms of a given minimum permissible $T_{\nu_e}^0$, which we designate $\mathcal{T}_{\nu_e}^0$; this is understood to refer to a limitation on the electron neutrino temperature provided independently of the neutrino data, such as may arise from supernovae modeling. If one cannot bound $T_{\nu_e}^0$ from below then the parameter $\sin^2 2\theta_V$ cannot be constrained. In order to rule out large vacuum angle solutions to the solar neutrino problem ($.7 \leq \sin^2 2\theta_V \leq .9$ [9]), using the SN1987A neutrino data, a rigorous argument that supernovae

²In our formalism E_{53}^B is determined by the combination of α , $T_{\nu_e}^0$ and τ_c , thus in the present context we obtain α from the fixed values of E_{53}^B and $T_{\nu_e}^0$ and the free value for τ_c .

dynamics *require* $T_{\nu_e}^0 > 4$ MeV appears to be needed. The $T_{\nu_e}^0$ parameters in Table 1 are well within the typical range of 3-5 MeV in the supernovae model literature [13, 14].

Conclusions

Our results demonstrate several important lessons for statistical analyses of constraints on neutrino properties from a nearby supernova neutrino burst, as well as refining these constraints for the observed burst from SN1987A. In the first place, while a Maximum Likelihood procedure can provide very powerful constraints on model parameters, it alone cannot address the question of whether these model parameters can be realistically achieved. When these parameters have to do with features of the observed burst, and not internal features of an underlying supernova model, then a Monte-Carlo procedure such as we have devised [4] can prove to be very useful in further strengthening constraints on neutrino properties.

Next, we have seen that the ability of the SN1987A burst signals in Kamiokande and IMB to constrain a non-zero electron neutrino mass is in some sense fortuitous, due to the “tension” of the Kamiokande and IMB data—in particular the apparent paucity of events in Kamiokande relative to IMB. For this reason, when we included deadtime in IMB we were able to further extend the lever-arm in constraining m_{ν_e} . Our final result, $m_{\nu_e} < 19.6eV$ is approximately 25% stronger than the previous best limit.

Finally, we find that the ability of the combined SN1987A neutrino bursts to constrain neutrino masses does not at present extend to an ability to constrain neutrino mixing angles in any model independent way. In particular, because of the uncertainty in the timescale for neutronization, without intro-

ducing strong model dependence—in particular constraints on E_{53}^B and $T_{\bar{\nu}_e}$ —one cannot limit $\sin^2 2\theta_V$ from the SN1987A neutrino events. This argues against the claim made in [8]. It will be interesting to determine just how strong the constraints might become for a galactic supernova burst, and this issue is currently under investigation.

We thank Steve Dye, Robert Svoboda and Martin White for useful conversations. We also thank the IMB collaboration for providing unpublished data.

References

- [1] C.B.Bratton *et al.* , Phys. Rev. D **37**, 3361 (1988)
R.M.Bionta *et al.* , Phys. Rev. Lett. **58**, 1494 (1987)
- [2] K.S.Hirata *et al.* , Phys. Rev. D **38**, 448 (1988)
K.S.Hirata *et al.* , Phys. Rev. Lett. **58**, 1490 (1987)
- [3] L.M.Krauss, Nature **329**, 689 (1987)
- [4] L.M.Krauss, P.Romanelli, D.Schramm, and R.Lehrer, Nucl. Phys. B. **380**, 507 (1992)
- [5] T.J.Loredo, and D.Q.Lamb, Ann. N.Y. Acad. Sci. **571**, 601 (1989)
- [6] Steve Dye, private communication
- [7] L.F.Abbot, A.De Rújula, and T.P.Walker, Nucl. Phys. B. **299**, 734 (1988)
- [8] A.Y.Smirnov, D.N.Spergel, and J.N.Bahcall, preprint hep-ph 9305204 (1993)
- [9] P.I.Krastev and S.T.Petcov, Phys. Rev. Lett. **72**, 1960 1994
P.J.Kernan, Ph.D.Thesis Ohio State University (1993)
S.L.Glashow and L.M.Krauss, Phys.Lett. **B190** 199 (1987)
V.Barger, K.Whisnant and R.J.N.Phillips, Phys. Rev. D **24** 538 (1981)
J.N.Bahcall and S.C.Frautschi, Phys. Lett. **B29**, 263 (1969)
B.Pontecorvo, Sov.JETP, **26** 984 (1968)

- [10] An excellent review is found in J.N.Bahcall, *Neutrino Astrophysics* (Cambridge University Press, Cambridge, 1989).
- [11] Particle Data Group, *Phys.Rev.***D50** 1173 (1994)
- [12] E.W.Kolb, A.J.Stebbins, and M.S.Turner, *Phys. Rev. D.* **35**, 3598 (1987)
- [13] R.Mayle, J.R.Wilson, and D.N.Schramm, *Ap.J.* **318**, 288 (1987)
- [14] A.Burrows, *Ann.Rev.Nucl.Sci.* **40**, 181 (1990)

Figure Captions

Figure 1: The projection of the log Maximum Likelihood onto the m_{ν_e} axis.

Figure 2: The Maximum Likelihood offset times for the IMB and Kamiokande detectors as m_{ν_e} is varied. For comparison the Maximum Likelihood supernovae cooling timescale is also shown.

Figure 3: The log likelihood as a function of the offset time in the Kamiokande detector for several values of m_{ν_e} . The horizontal line indicates the 95% C.L. boundary.

Figure 4: Shown are Monte Carlo generated cumulative probability distributions for the time of the first event in a detector given the supernovae model parameters. In (a) the neutrino mass is 21 eV, and the distributions for IMB and Kamiokande are shown. The Maximum Likelihood offset times are also indicated. In (b) the neutrino mass is 19.6 eV. The distribution for Kamiokande is shown, as are the Maximum Likelihood and 95% C.L. offset times. The short horizontal line is at P=95%.

Figure 5: The projection of the log Maximum Likelihood onto the $\sin^2 2\theta_V$ axis.

Figure 6: Temporal profiles of the Maximum Likelihood electron, anti-electron, and muon neutrinosphere temperatures for mixing angles of $\sin^2 2\theta_V = 0$ (a), $\sin^2 2\theta_V = .45$ (b) and $\sin^2 2\theta_V = 1$ (c).

Figure 7: As a function of neutrino mixing angle, the Maximum Likelihood neutron star binding energy in units of 10^{53} ergs (a), initial electron neutrinosphere temperature in MeV (b), and supernovae neutrinosphere cooling timescale in seconds (c).

Figure 8: Maximum Likelihood Projections into the plane of the neutron star binding energy and initial electron neutrinosphere temperature for several choices of the neutrino mixing angle. The binding energy is in units of 10^{53} ergs and the temperature in MeV. The contours are displayed at the 95%, 50%, 25% and 10% Confidence Levels. For $\sin^2 2\theta_V = 1$ the 10% C.L. contour does not exist. For $\sin^2 2\theta_V = .1$ the 25% and 10% C.L. contours do not exist. (See Figure 5).

Table 1 : Maximum $T_{\nu_e}^0$ on the 95% C.L. boundaries of Figure 8

$T_{\nu_e}^0$ (MeV)	$\sin^2 2\theta_V^{95}$
3.59	1.0
3.67	0.9
3.96	0.7
4.27	0.5
5.00	0.25

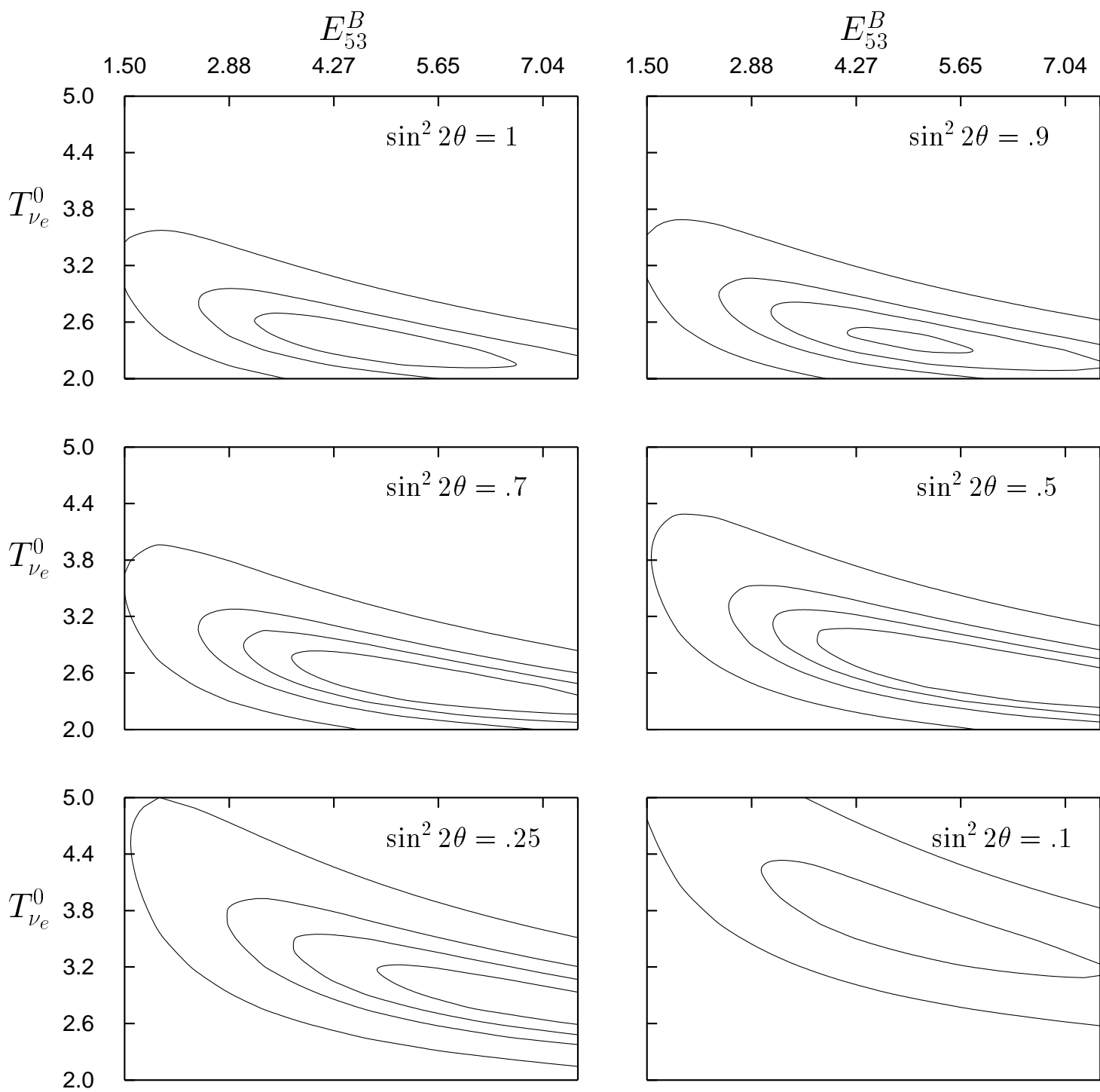


Figure 8

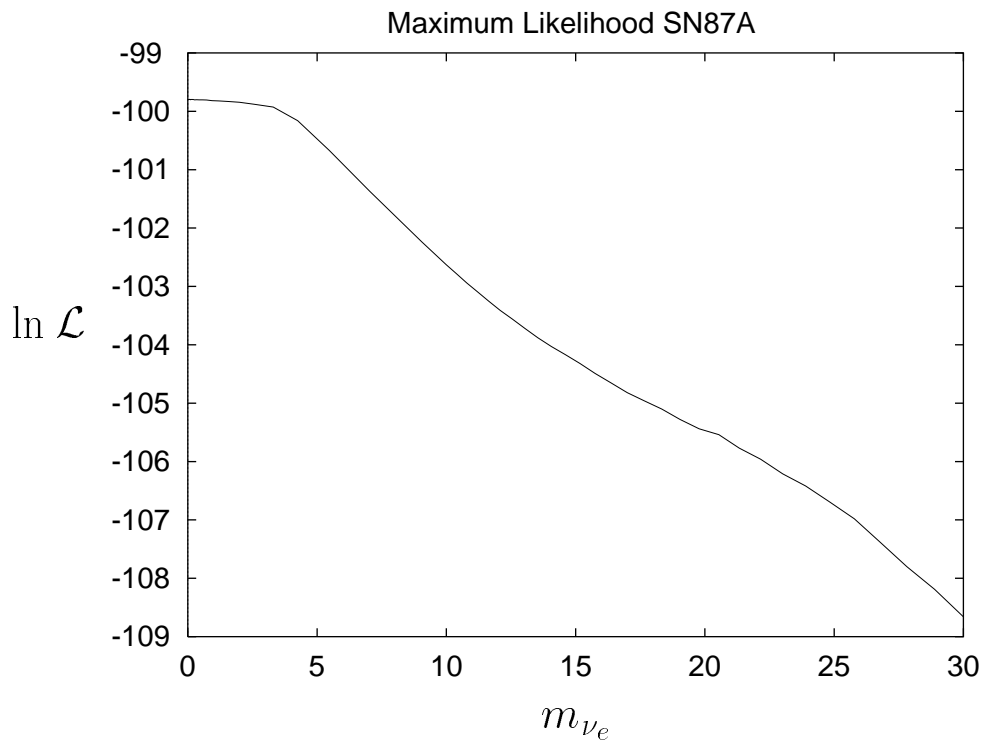


Figure 1

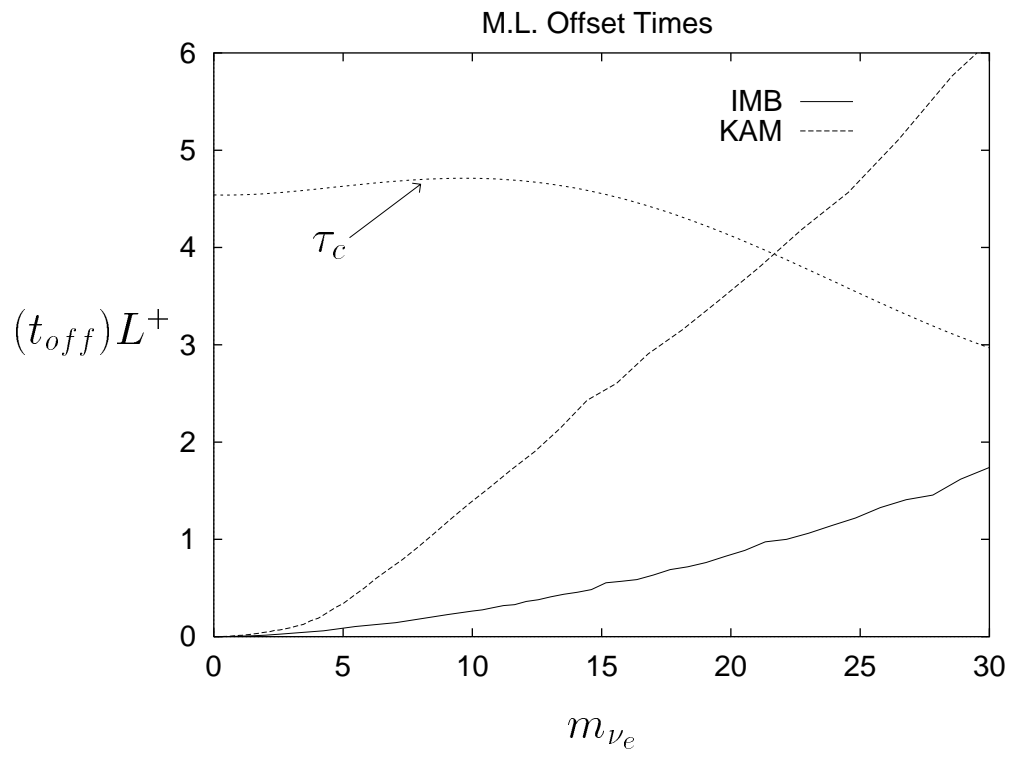


Figure 2

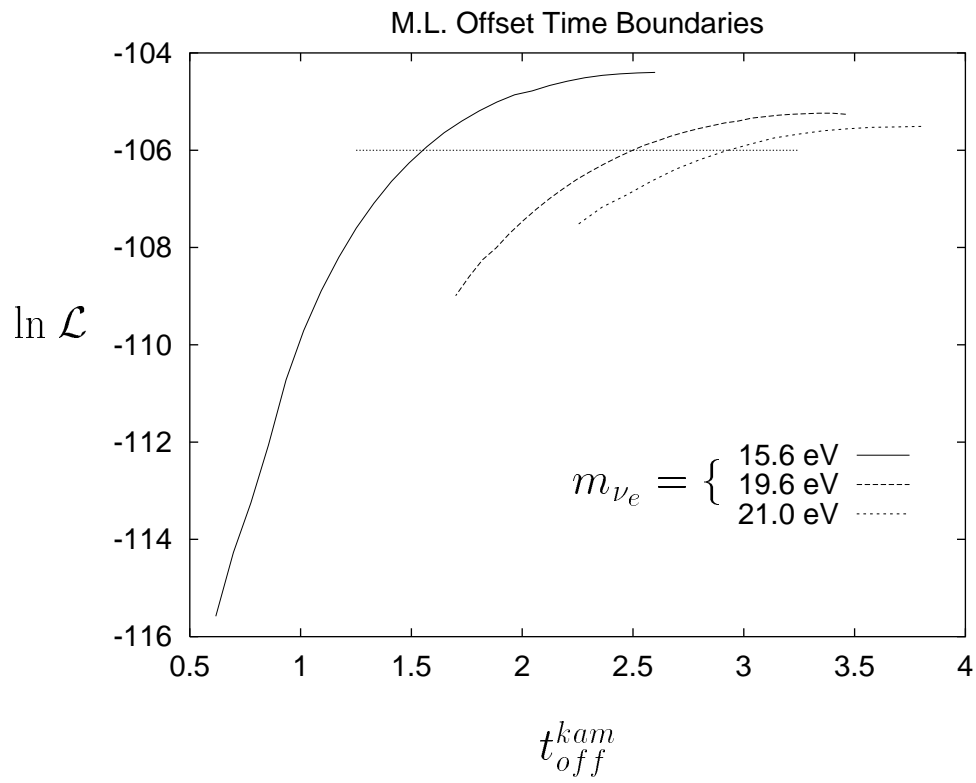


Figure 3

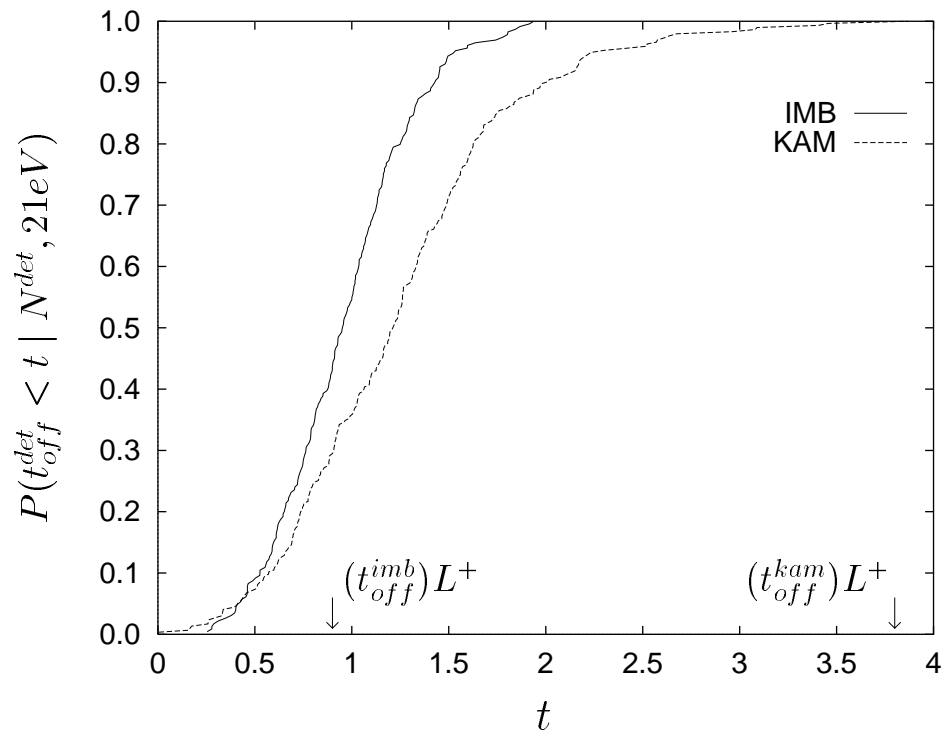


Figure 4a

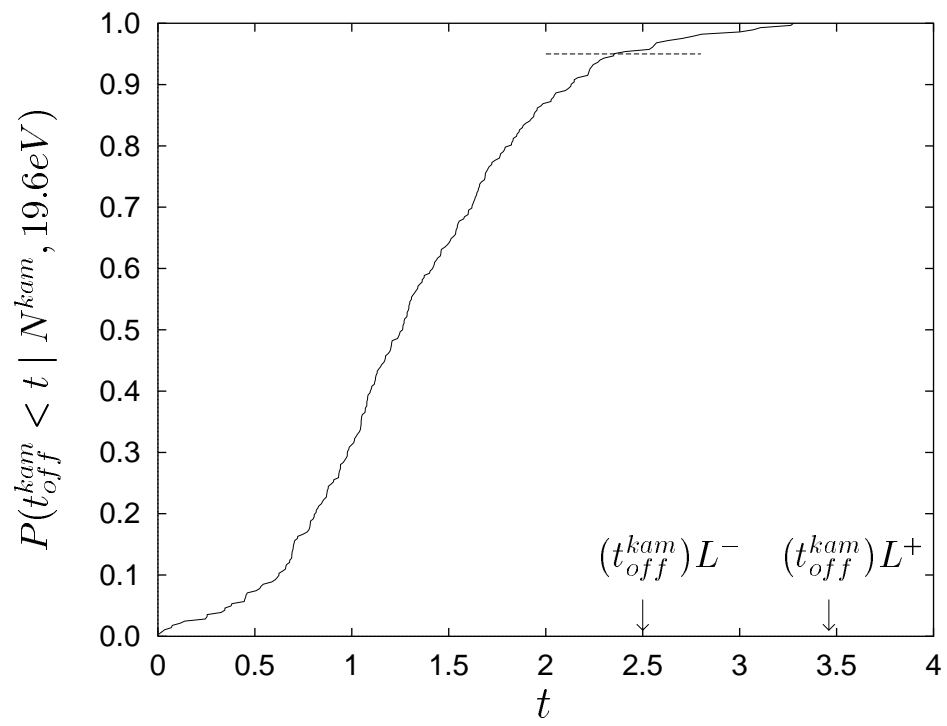


Figure 4b

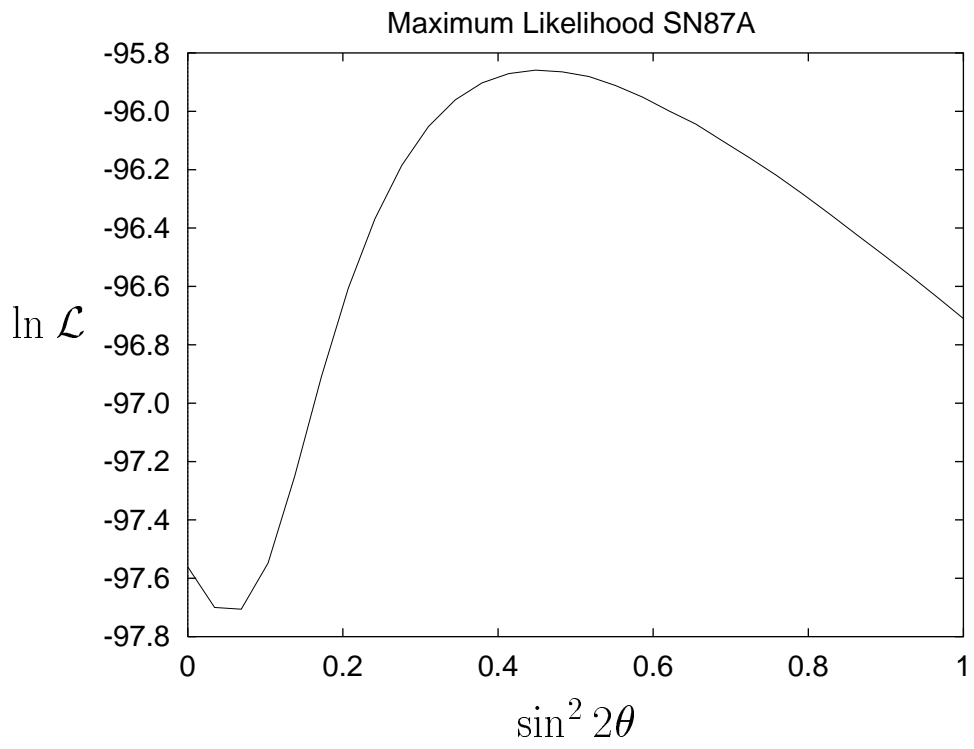


Figure 5

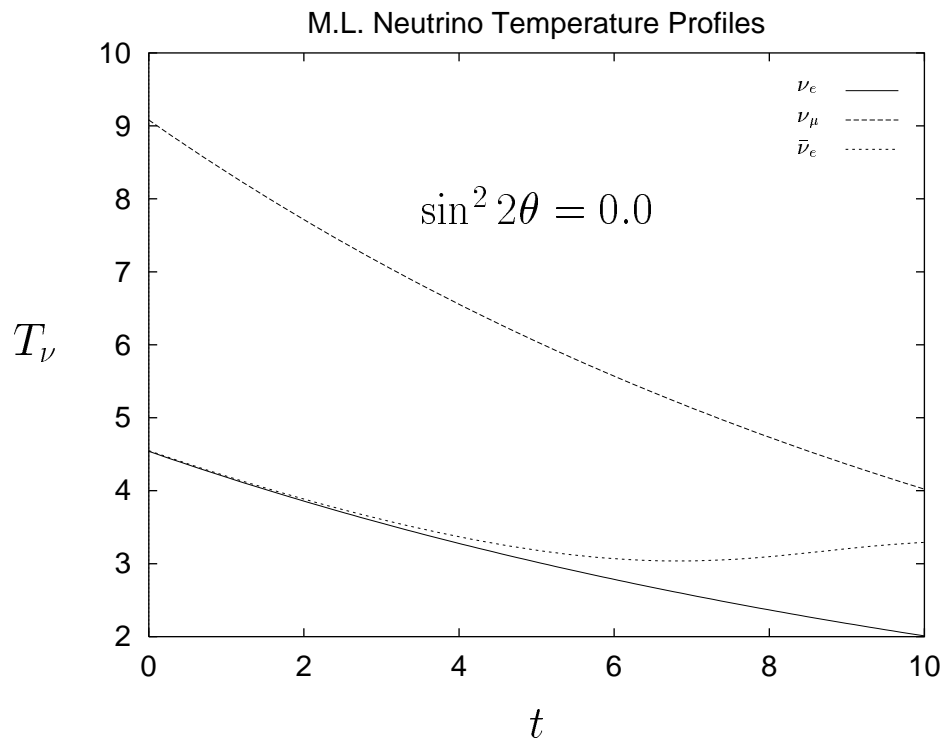


Figure 6a

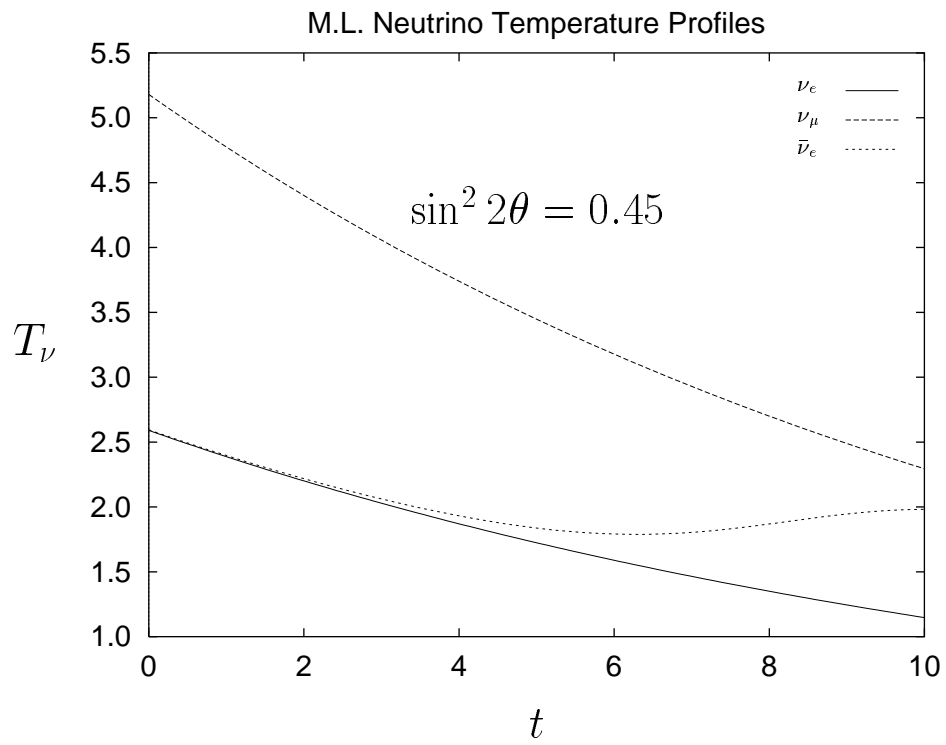


Figure 6b

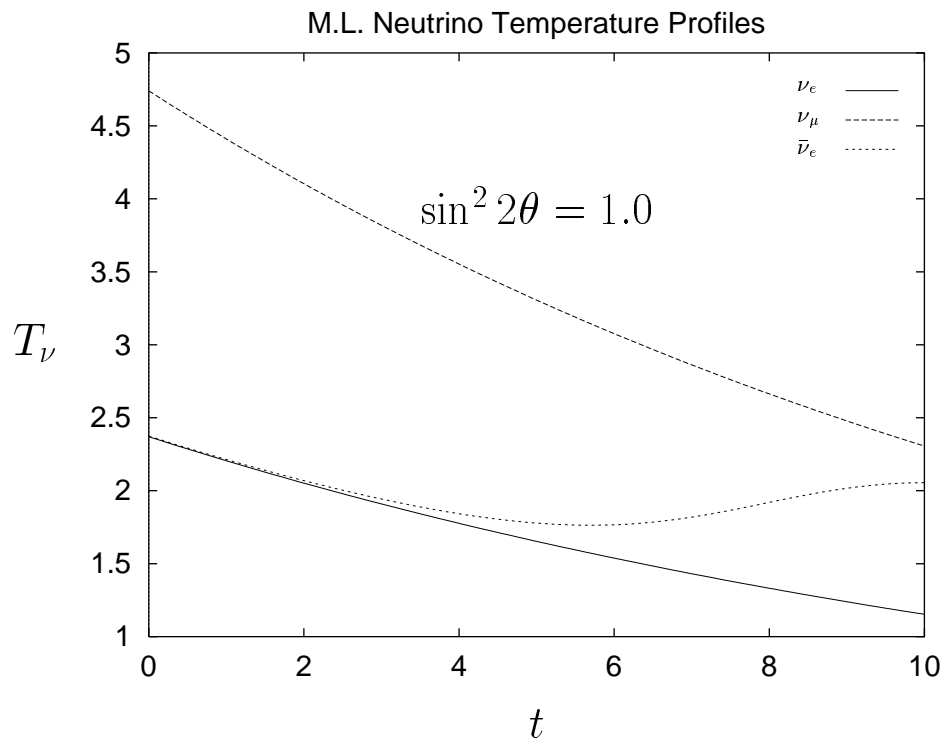


Figure 6c

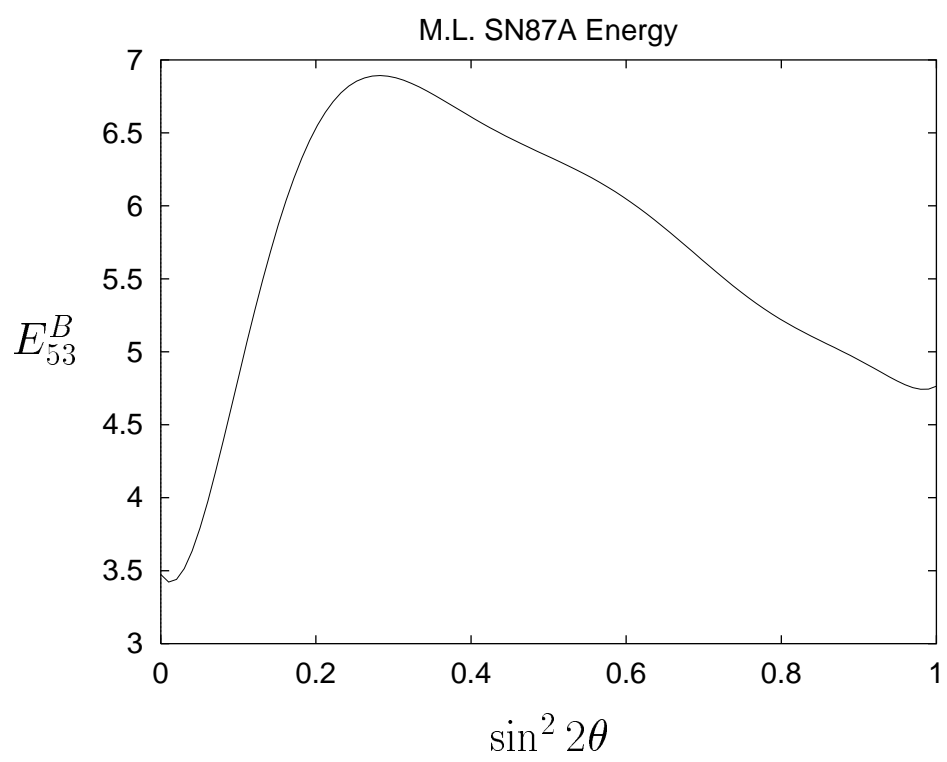


Figure 7a

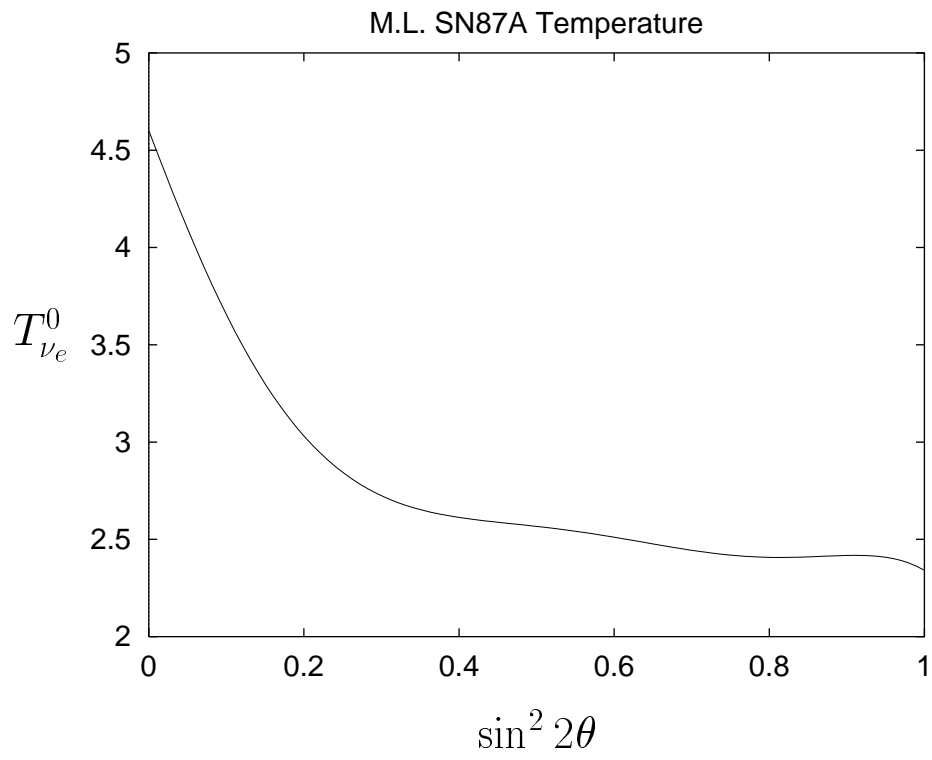


Figure 7b

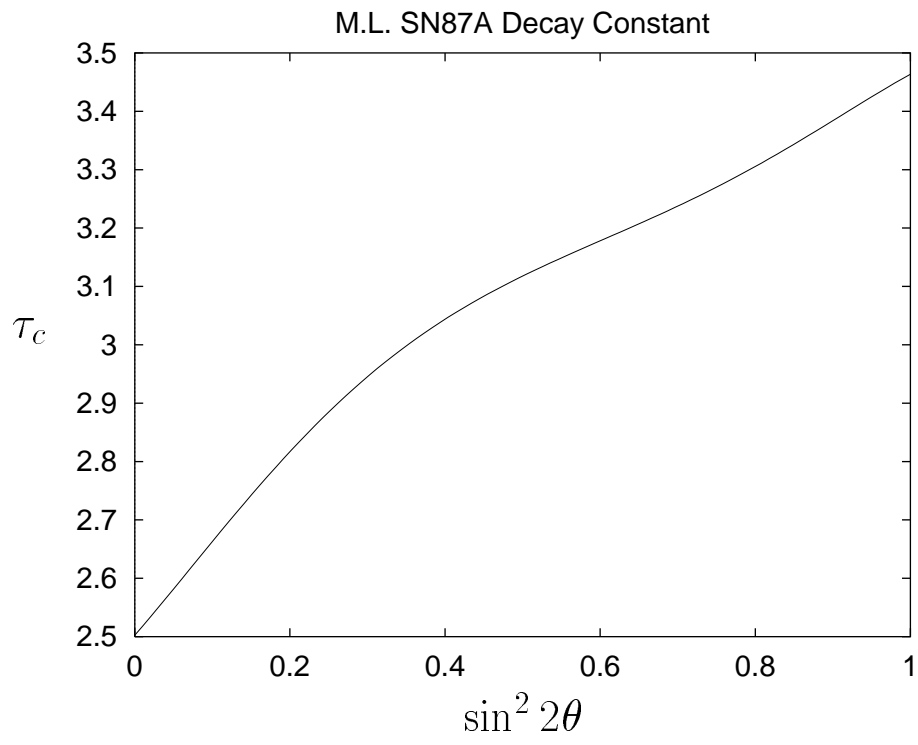


Figure 7c